Experimental investigation of shell-side steam pressure drop in crossflow in a horizontal falling-film tube bundle

S Q Shen [1]**, H Liu, L Y Gong, X S Mu and R Liu**
Key Laboratory for Sea Water Desalination of Liaoning Province, Dalian University of Technology, Dalian 116024, Liaoning, China

E-mail: zzbshen@dlut.edu.cn

Abstract. An experimental investigation of the steam flowing across a horizontal tube bundle with liquid falling film was conducted to simulate flow characteristics in a large desalination plant. Experiments were conducted at pressure ranging from 12 kPa to 31 kPa with the corresponding saturated steam temperature of 50 °C to 70 °C and the falling film spray density of 0.02 $kg \cdot m^{-1} \cdot s^{-1}$ to 0.08 $kg \cdot m^{-1} \cdot s^{-1}$. The influence of the spray density, saturated temperature and tube bundle geometry structure on steam pressure drop was illustrated. The results indicate that the pressure drop increased with increasing spray density, but decreased with increasing saturated temperature. The pressure drop at the maximum spray density of 0.08 $kg \cdot m^{-1} \cdot s^{-1}$ can be three times that in spray density of 0.02 $kg \cdot m^{-1} \cdot s^{-1}$ and the pressure drop at 50 °C is almost twice that at 70 °C. Under the same condition, the pressure drop through a rotated square-arranged tube bundle was smaller than that through a regular triangular-arranged tube bundle.

1. Introduction

The horizontal tube falling-film evaporator is a high-efficiency heat transfer equipment with wide applications in chemical engineering, refrigeration and seawater desalination plants. Most studies on the process of horizontal tube falling film evaporators focus on the heat transfer coefficient [1, 2]. Parameters such as the liquid film Reynolds number, evaporation temperature, liquid properties, tube space and heat flux have been studied as the major parameters that affect heat transfer performance. Ribatski et al. [3] presented a critical review of research on horizontal tube falling film evaporators before 2005. Shen et al. [4] showed the uneven distribution of heat transfer within a large-scale tube falling-film evaporator considering the heat transfer coefficient distribution, which is affected by the spray density and condensation in tubes.

Pressure drop is a critical parameter for the heat transfer performance of the multi-effect distillation (MED) desalination plant for its dominant function in the calculation of temperature loss [5, 6]. The thermal process in horizontal tube falling film evaporators in MED is characterised by the small temperature difference, minimal pressure drop, high sensitivity and saturation state.

The functional relationship between the pressure drop and relevant variables are determined experimentally. Based on an experimental databank, Fujii et al. [7] studied the effect of in-line and staggered arrangements of tube banks on the pressure drop coefficient. The lack of reliable method for predicting the void fraction motivated Grant and Chisholm [8] to establish a new equation for shell-side two-phase pressure drop using their data. Ribatski et al. [9] analysed and summarized previous

[1] zzbshen@dlut.edu.cn.

researches on the two-phase flow. They critically described the frictional pressure drop, the prediction methods of which are generally based on experimental results of the adiabatic air-water flow. Ishihara et al. [10] suggested a Martinelli model-based correlation approach to represent the two-phase pressure drop friction multiplier. Since then, researches on two-phase pressure drop in tube banks are mainly been based on this correlation. Some relative factors, such as the tube pitch [11]; flow pattern [12] and void fraction [13, 14] have been gradually integrated to improve the correlation.

The flow in horizontal tube falling film evaporators is complex and differs from general two-phase flow. Such flow contains a downward falling film flow driven by the gravity and a steam flow across the tube bundle driven by pressure difference. The pressure drop of the steam flowing across tube bundle is caused not only by the tube bundle, but also by the falling liquid. However, the effect of liquid film on pressure drop is not considered in the aforementioned studies. This paper aims to experimentally investigate the characteristics of steam flowing across the falling-film tube bundle and to determine the effect of liquid film on steam pressure drop.

2. Experiment and error analysis

2.1Experimental apparatus and procedure

Figure1 shows the experimental system for the steam pressure drop in the horizontal-tube falling-film evaporator. The system consists of a boiler to provide steam, a temperature & pressure reducer to control the saturated steam pressure and temperature, a test section with a tube bundle and a water spray box, a condenser, water reservoirs, pumps and measuring instruments.

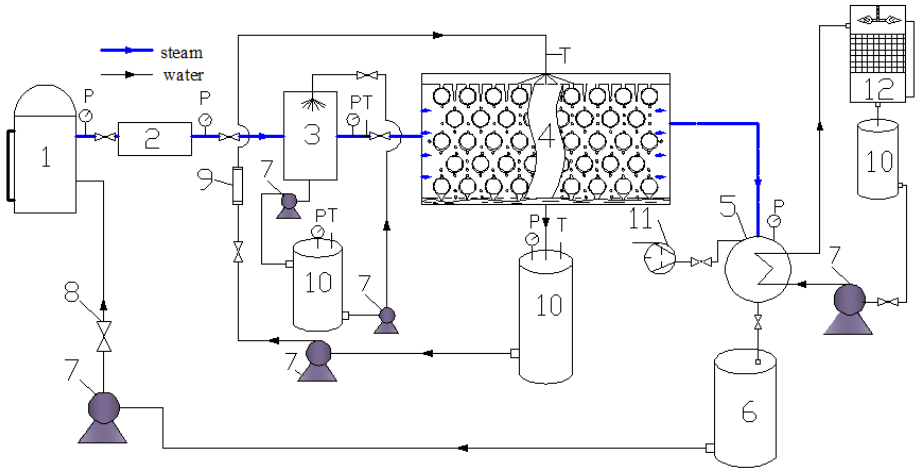

1 - Boiler 2 - Steam distributing cylinder 3 - Temperature and pressure reducer
4 - Test section 5 - Condenser 6 - Condensate tank
7 - Water pump 8 - Valve 9 - Float flow meter 10 - Water reservoir
11 - Vacuum pump 12- Cooling tower P - Pressure gauge T - Thermocouple

Figure 1. Experimental system diagram.

In each experiment, a designed amount of steam was generated from the boiler and flows through the tube bundle with falling film flow under adiabatic condition. After flowing across the tube bundle, the steam flowed into the condenser, where it was condensed into water and then pumped back to the boiler for recycling. The required steady flow rate of saturated water was controlled by the associated pump at the water reservoir to distribute over the top row of tubes to form falling films. After flowing downward through the tube bundle continuously, the saturated water flowed to the water reservoir for recycling. An electrical bar was employed as the heating source in water reservoir to maintain the temperature of saturated water. The system pressure was maintained by the vacuum pump and condenser.

The test section is illustrated in figure 2. The inlets and outlets of the test section are equipped with thermocouples to measure the fluid temperatures. Pressure and pressure difference sensors are installed in the inlet and outlet of the tube bundle. The quantity of saturated water supplied by the pump is measured by a rotameter whereas the fluid temperature is measured by a T-type armoured thermocouple.

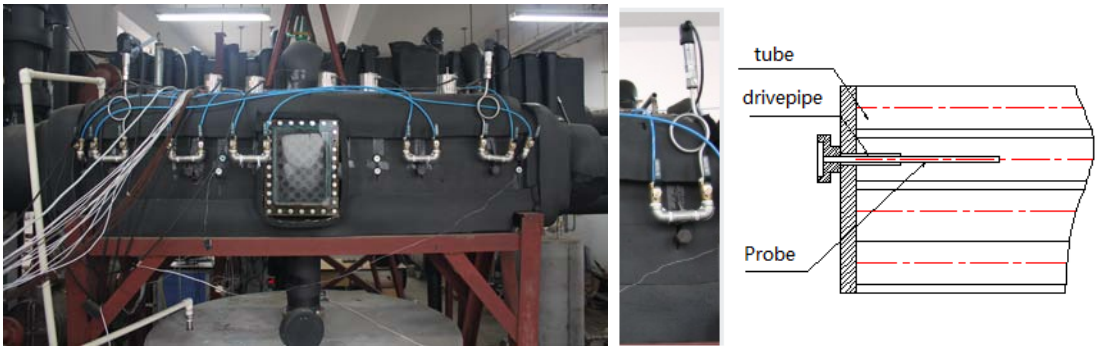

Figure 2. Image of test section and installation of test instrument.

Tube bundles consist of Al-brass tubes with 0.0254m outer diameter and 0.5 m long; with the tube pitch 1.3 times the outer diameter. As shown in figure 3, two types of arrangement, the regular triangle and rotated square arrangements are selected, for which the number of tubes are 501 and 448, respectively. The minimum cross-section area at the vertical surface across the centre of a tube row is taken as the calculation flow area.

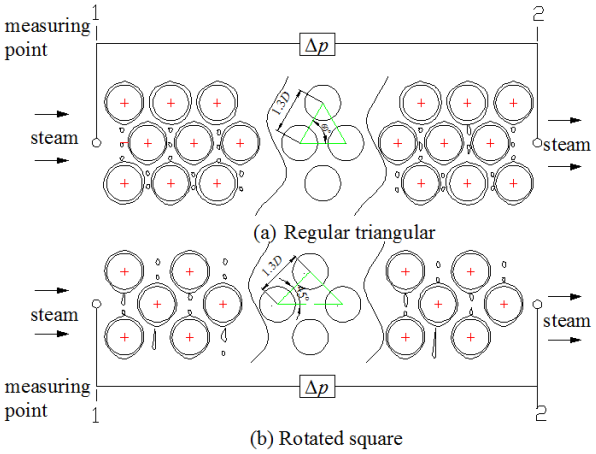

Figure 3. Diagram of tube bundle arrangement.

2.2 Experimental condition and error analysis

In the early stage of each experimental condition, the steam flow rate is changing and not stable, so the measuring result is not steady. The metering begins until the measured parameters are steady to ensure the accuracy. The quantity of falling-film flow is measured by the unilateral spray density Γ. The steam mass flow rate (per area) G is calculated by the minimum cross-section area and employed by the weight of condensed water. The ranges of experimental parameters are given in Table 1. The float of the experimental data is within the estimate range and thus acceptable.

Table1. Experimental conditions

Name	Regular Triangle	Rotated square
T /°C	50–70	50–70
P /kPa	12–31	12–31
G /kg·m^{-2}·s^{-1}	0.19–1.1	0.39–1.24
Γ/kg·m^{-1}·s^{-1}	0.02–0.08	0.02–0.08

The precision of the pressure difference sensor (GE Druck LPX9381) is ±1 Pa with the measuring range from 0 Pa to 1000 Pa. The precision of the pressure sensor (UNIK PMP5073) is 0.03 kPa with the measuring range from -0.1 MPa to 0 MPa (gauge pressure). The water flow rate is measured by using rotameters (LZB-80) with the measuring range from 2 m3/h to 20 m3/h and 2% precision. The operating temperature from 50 °C to 70 °C is measured by T-type armoured thermocouples with the precision of ±0.05 °C. The sensors are calibrated before the experiment. The measuring signal is collected by a National Instruments (NI) controller PXI-1042. Software, Lab VIEW (NI, Austin, Texas, USA), makes the data visible when they are saved. Measurements are performed under adiabatic conditions.

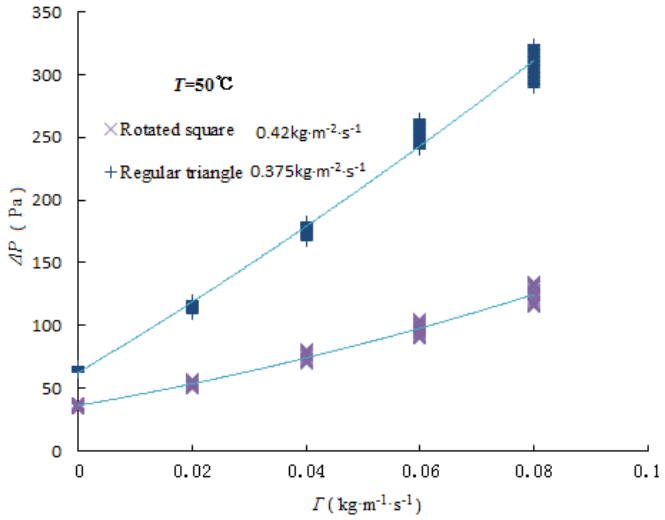

Figure 4. Distribution of data.

Each signal of T, p and Δp is processed by the acquisition system and stored in computer. Under stable experimental conditions, no less than 50 numbers were recorded for each set of parameters. Figure 4 takes some certain conditions to illustrate the experimental data. Owing to the high instrumental sensitivity and the small change in each experimental condition, the metering data varies and hold wave in the vicinity of a value. In each certain condition, the metering data contains more than 50 values. The fluctuate of each set data is within 5%, which shows good steadiness. The average value in each condition will be employed in the following discussion.

Tube bundles consist of Al-brass tubes with 0.0254 m outer diameter and 0.5 m long; with the tube pitch 1.3 times the outer diameter. As shown in figure 3, two types of arrangement, the regular triangle and rotated square arrangements are selected, for which the number of tubes are 501 and 448, respectively. The minimum cross-section area at the vertical surface across the centre of a tube row is taken as the calculation flow area.

3. Results and Analysis

The pressure drop of each column tube $\overline{\Delta p}$ is chosen to characterize the flow resistance in the comparison of different tube arrangements. Figure 5 shows the variation of pressure drop with the spray density and saturated temperature in the regular triangle arrangement.

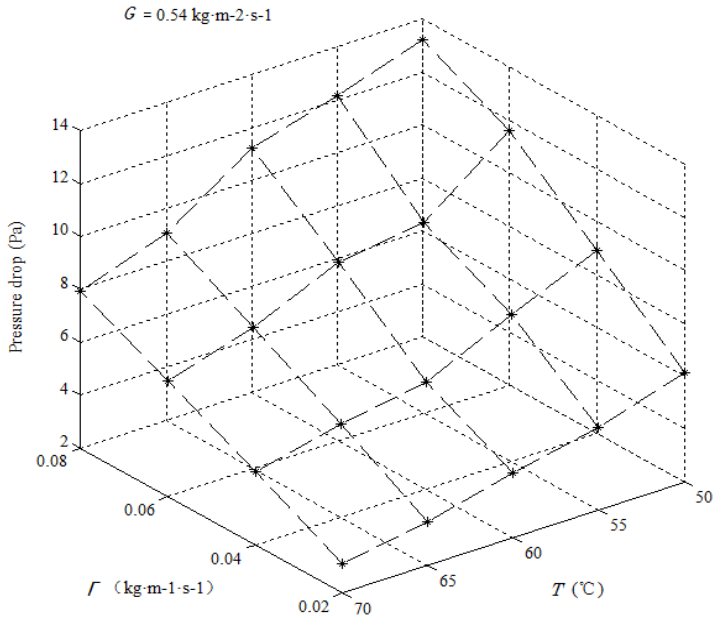

Figure 5. Pressure drop in regular triangle arrangement.

Figure 5 shows that in the range of spray density Γ. On average, $\overline{\Delta p}$ will increase by approximate 2 Pa for every 0.02 kg·m^{-1}·s^{-1} increment of the spray density. Considering different T values, in Γ=0.08 kg·m^{-1}·s^{-1} is two to three times than that of Γ=0.02 kg·m^{-1}·s^{-1}.

The experimental results show that the spray density affects the flow resistance significantly when the steam flows across tube bundle. When liquid sprayed on the tube forms a falling-film outside the tube surfaces, the tube outer diameter increases whereas the tube pitch decreases. This causes the actual flow velocity to become higher than the calculated superficial value. Consequently, the pressure drop, as well as the speed and frequency of droplets between the tubes, will increase with the increasing spray density. When spray density increases to a certain degree, the original falling-film mode of the droplet gradually changes into the jet mode, as illustrated by Armbruster [1] and Hu [16]. This mode further reduces the flow area and increases the actual flow velocity between tubes. Furthermore, the existence of the droplet and liquid film will increase the additional contact area between steam and liquid and thereby increase the frictional resistance. In a word, the pressure drop increases with the increasing of spray density.

Figure 5 also shows that pressure drop decreases with increasing temperature. $\overline{\Delta p}$ at 50 °C is nearly twice that at 70 °C. In a constant G, saturated steam density increases with temperature. Thus, the smaller steam velocity occurs at higher temperature. The impact factor of steam velocity on pressure drop is higher than that of steam density. Therefore, a higher temperature results in a smaller pressure drop. Furthermore, water dynamic viscosity is low at high temperature, which will cause the friction resistance become small at high temperature when steam flows across the falling-film tube. Therefore, pressure drop decreases with increasing temperature.

Figure 6 shows the pressure drop in the rotated square tube bundle arrangement. The tendency of pressure drop is similar to that in regular triangular arrangement as shown in figure 5. However, the value in rotated square tube bundle is obviously small.

The falling film evaporation occurs in an actual evaporator, such that the spray density changes along the vertical direction. Spray density actually decreases gradually along the downward direction. Based on the data of pressure drop illustrated in figures 5 and 6 and the above description of pressure drop change law, we can image the distribution of pressure in evaporator and the coefficient of pressure drop decreases gradually along the tube row direction.

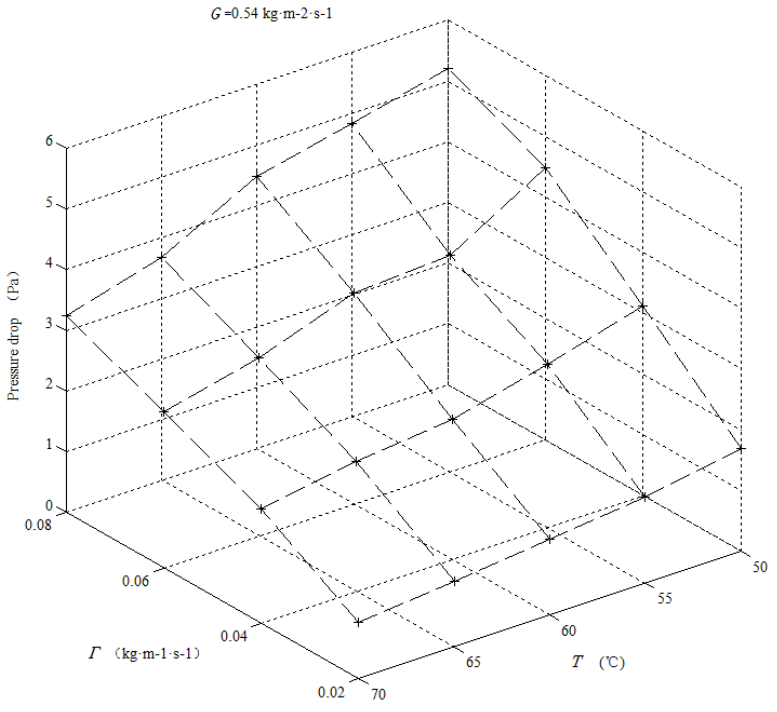

Figure 6. Pressure drop in rotated square arrangement.

A MED system has many effect-evaporators and the steam mass flow rate generated outside of tube in each effect-evaporator is approximately the same. The working pressure and corresponding temperature decrease with the evaporator effect number. Experimental data show that pressure drop decreases with increasing temperature. In other words, the change of temperature in experiment can be regarded as the effect number of the multi-effect evaporation device. The data of pressure drop and its change with the temperature can indicate that the pressure drop in a low-temperature-effect evaporator is higher than that in a high-temperature-effect evaporator.

R is defined to evaluate the effect of tube bundle configuration on pressure drop as follows:

$$R=\frac{\overline{\Delta p}_{\mathrm{RT}}}{\overline{\Delta p}_{\mathrm{RS}}} \tag{1}$$

where $\overline{\Delta p}_{\mathrm{RT}}$ represents the pressure drop in regular triangle arrangement; $\overline{\Delta p}_{\mathrm{RS}}$ represents the pressure drop in rotated square arrangement.

The ratio (R) between $\overline{\Delta p}$ in regular triangle and rotated square arrangements is illustrated in figure 7. The value of R more than 2.5 shows that the pressure drop in regular triangle is obviously high than that in rotated square arrangements. Although same the both relative tube pitch in two arrangements, the adjacent vertical and horizontal tube pitch are different because of the tube bundle

geometry structure. The effect of tube bundle geometry structure on pressure drop is analysed in two aspects. 1) Compared with the rotated square arrangement, the vertical adjacent tube pitch of the regular triangle arrangement is longer. Under the same spray density, the velocity of liquid droplet or falling film among the vertical adjacent tubes, as well as the velocity of liquid film outside the tube is higher in regular triangle arrangement. When steam flows through the tube bundle, the friction resistance and shear force of steam occurs with the liquid droplet or falling film among the vertical adjacent tubes as well as with the liquid film outside the tube. Thereby, the higher velocity causes the bigger pressure drop. 2) The horizontal adjacent tube pitch of the regular triangle arrangement is shorter than that of rotated square arrangement, which will cause the steam flow worse in horizontal direction. In comparison, the steam flow is more frequent change in the regular triangle arrangement; consequently the local resistance is much bigger. In all, the pressure drop in regular triangle is higher than that in rotated square arrangements.

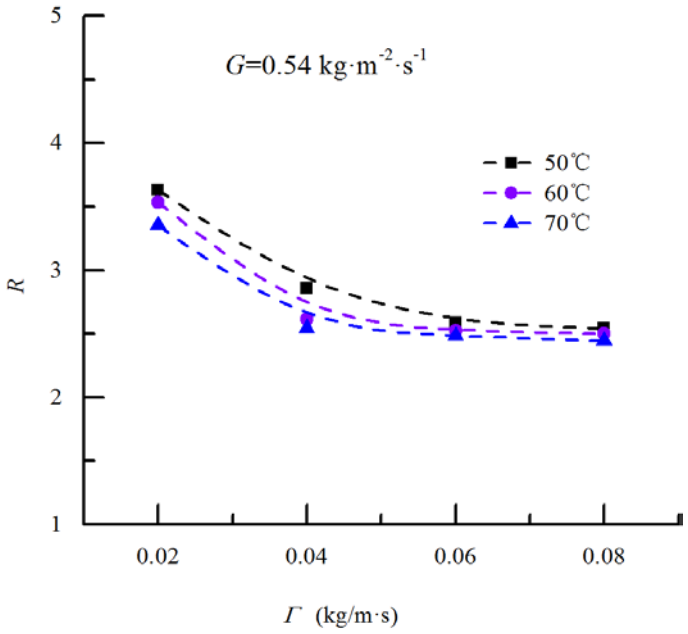

Figure 7. Ratios of pressure drop in two arrangements.

When temperature changes from 50 °C to 70 °C, the change of R is little. With increasing spray density R decreases, nevertheless, the change trend becomes small and it maintains stable. When spray density is 0.02 kg·m^{-1}·s^{-1}, R is more than 3; when spray density increases to 0.04 kg·m^{-1}·s^{-1}, it reduces to 2.8; from 0.06 kg·m^{-1}·s^{-1} to 0.08 kg·m^{-1}·s^{-1}, R maintains about 2.5. At a small spray density, the flow pattern among the vertical adjacent tubes is drop-wise flow; the development and breakup of liquid pendant and droplet are more intense in long vertical adjacent tube pitch. Thus, the value of R is higher at a small spray density. Given that droplets grow with increasing spray density, the liquid flow pattern turns into the jet mode [1, 15]. The effect of spray density on steam horizontal flow changes little. Thus, the R maintains stability from 0.06 kg·m^{-1}·s^{-1} to 0.08 kg·m^{-1}·s^{-1}.

4. Conclusions

Experiments were conducted to measure the pressure drop under the condition of steam flow across the horizontal tube bundle with falling-film flow. Experimental results determine the law for pressure drop with tube bundle structure, column number, temperature and spray density. The conclusions are as follows:

1) For a horizontal tube falling film evaporator, spray density has a significant influence on pressure drop. The pressure drop at the maximum spray density of 0.08 $kg \cdot m^{-1} \cdot s^{-1}$ can be three times that in spray density of 0.02 $kg \cdot m^{-1} \cdot s^{-1}$.
2) The saturated temperature also affects the pressure drop. Under the same steam flow rate, the pressure drop at 50 °C is almost twice that at 70 °C.
3) The tube bundle structure has an obvious effect on pressure drop. The rotated square arrangement is more conductive to the steam flowing across a horizontal falling-film tube bundle and the pressure drop in that is smaller.

5. References

[1] Armbruster R and Mitrovic J 1998 *Exp. Therm. Fluid Sci.* 18 183-194
[2] Liu Z H and Yi J 2002 *Appl.Ther. Eng.* **22** 83-95
[3] Ribatski G and Jacobi A M 2005 *Int. J. Refrig.* **28** 635-653
[4] Shen S Q, Liang G T and Gong L Y 2011 *CIESC J.* **62** 3381-85
[5] Hisham T E, Imad A, Bingulac S and Ettouney H 1998 *Chem. Eng. Technol.* **28** 437-451
[6] Hisham T E, Ettouney T, Hisham M E and Faisal M 2000 *Appl. Therm. Eng.* **20** 1679-1706
[7] Fujii T, Uehara H, hirata K and Oda K 1972 *Int. J. Heat Mass Trans.***15** 247-260
[8] Grant I D R and Chisholm D 1979 *J. Heat Trans.-T. ASME* **101** 38-42
[9] Ribatski G and Thome J R 2007 *Heat Transfer Eng.* **28** 508-524
[10] Ishiraha K, Palen J W and Taborek J 1980 *Heat Transfer Eng.***1** 23-32
[11] Dowlati R, Kawaji M and Chan A M C 1990 *AIChE J.* **36** 765-772
[12] Xu G P, Tso C P and Tou K W 1998 *J. Fluid Eng.-T. ASME* **120** 140-145
[13] Dowlati R, Kawaji M and Chan A M C 1996 *J. Heat Trans.-T. ASME* **118** 124-131
[14] Feenstra P A, Weaver D S and Judd R L 2000 *Int. J. Multiphase Flow* **26** 1851-73
[15] Hu X and Jacobi A M 1998 *Exp. Therm. Fluid Sci.* **16** 322-331
[16] Hassan A M 2010 *Energ. Convers. Manage.* **51** 703-709
[17] Liu H, Shen S Q, Gong L Y and Chen S 2014 *Appl. Therm. Eng.* **69** 214-220

6. Acknowledgments

This work is supported by the project of Chinese National Natural Science Foundation (No. 51336017). The authors are grateful for the financial support